

Supercritical Fluid Processing of Nafion[®] Membranes: Methanol Permeability and Proton Conductivity

Juan C. Pulido Ayazo, David Suleiman

Chemical Engineering Department, University of Puerto Rico, Mayagüez, PR 00681-9000

Received 26 May 2011; accepted 12 June 2011

DOI 10.1002/app.35098

Published online 3 October 2011 in Wiley Online Library (wileyonlinelibrary.com).

ABSTRACT: Nafion[®] membranes commonly used in direct methanol fuel cells (DMFC) are typically limited by high methanol permeability. These membranes have phase-segregated sulfonated ionic domains in a perfluorinated backbone, which make processing difficult and limited by phase equilibria considerations. This study used supercritical fluids (SCFs) as a processing alternative, since the gas-like mass transport properties of SCFs allow for better penetration into the membranes and the use of polar cosolvents could also influence their morphology, thus fine-tuning their physical and transport properties. The SCF processing was performed at 40°C and 200 bars using pure CO₂ and CO₂ with several polar cosolvents of different size and chemical functionalities like: acetic acid, acetone, acetonitrile, cyclohexanone, dichloromethane, ethanol, isopropanol, methanol, and tetrahydrofuran. Methanol permeability measurements revealed that the SCF processed membranes reduced the permeation of methanol by several orders of magnitude, especially with

the use of some small polar cosolvents. Proton conductivity measurements, using AC electrochemical impedance spectroscopy, were on the order of 0.03–0.09 S/cm, which indicates that processing with SCF CO₂ plus some cosolvents maintained the high proton conductivity while reducing the methanol permeability. The results are explained using XRD and SAXS. XRD analysis of the SCF processed samples revealed an increasing pattern in the crystallinity, which influenced the transport properties of the membrane. SAXS measurements confirmed the morphological differences that led to the changes in transport properties of the SCF processed membranes. Finally, processing flow direction (parallel versus perpendicular flow) played a major role in the morphological changes of this anisotropic membrane. © 2011 Wiley Periodicals, Inc. *J Appl Polym Sci* 124: 145–154, 2012

Key words: nafion[®]; supercritical fluids; PEM; DMFC; XRD; SAXS

INTRODUCTION

Despite all the advances in the development of proton exchanged membranes (PEM) for fuel cell applications, Nafion[®] remains the most commonly used PEM for direct methanol fuel cells (DMFC). Nafion[®] is a noncrosslinked ion exchange polymer (ionomer) with a perfluorinated backbone and sulfonate ionic groups attached to perfluorovinylether side chains. The semicrystalline structure of Nafion[®] is separated into two microphases: a hydrophobic perfluorinated region (backbone) and hydrophilic domains formed by the ionic clusters. Nafion[®] has excellent resistance to chemicals due to the perfluorinated backbone, and high proton conductivity caused by the sulfonic

groups. Unfortunately, since the transport mechanism for protons and methanol is very similar (from sulfonic group to sulfonic group in the presence of water), it has the problem of the methanol crossover from the anode to the cathode; which reduces the cathode potential and decreases the cell efficiency. Over 40% of the methanol used in the DMFC can be wasted across Nafion[®] membranes.¹

Different authors have investigated ways to modify Nafion[®], with the goal of decreasing the methanol crossover, while maintaining the proton conductivity high and therefore increase the performance and efficiency of the DMFC. The most common approaches involve creating Nafion[®] hybrid membranes² (e.g., organic or inorganic fillers, acid–base blends, and polymer–ceramic membranes) to change the polymer chemistry and pursue different transport mechanisms throughout the membranes; therefore, reducing the methanol permeability. Unfortunately, most of the Nafion[®]-based hybrid approaches also decrease the proton conductivity similar to the reduction in methanol permeability.^{2–4}

Solvent effects have also been studied to pursue morphological changes in Nafion[®] membranes. One of such study used small polar protic solvents (e.g., methanol,

Correspondence to: D. Suleiman (david.suleiman@upr.edu).

Contract grant sponsor: Department of Defense of the United States; contract grant numbers: DAAD19-03-1-0141, W911-NF-07-10244.

Contract grant sponsor: University of Washington; contract grant number: NSF DMR 0817622.

TABLE I
Selected Physical Properties of Cosolvents Used with SCF CO₂⁶

Cosolvent	Solubility Parameter (δ) (Cal/cm ³) ^{1/2}	Dipole Moment (μ) (D)	Dielectric Constant (ϵ) (De)	Molar Volume (v_i) (cm ³ /mole)
Acetic acid	10.1	1.74	6.2	57.2
Acetone	9.9	2.88	20.7	73.5
Acetonitrile	11.9	3.92	36.6	52.3
Cyclohexanone	9.9	3.01	18.2	103.6
Dichloromethane	9.7	1.60	9.1	64.0
Ethanol	12.7	1.69	24.3	58.4
Isopropanol	8.8	1.68	20.1	76.5
Methanol	14.5	1.70	33.0	40.5
Tetrahydrofuran	9.1	1.63	7.5	81.1

ethanol, 2-propanol, and water). Proton conductivity results showed a reduction in the alcohol environment, while the aqueous environment maintained the high values commonly found in Nafion[®]; unfortunately, the study did not include methanol permeability.

Several alternatives to Nafion[®] have also been considered such as: polyether ether ketone (PEEK),⁶ polysulfone,⁷ polybenzimidazole^{8,9} and poly(styrene-isobutylene-styrene).¹⁰ In addition, hybrid membranes of these and other membranes (e.g., organic-inorganic fillers, acid-base blends) have also been studied.^{8,9,11} Some of these membranes are promising candidates for DMFC applications.

For most of these membranes the transport of ions has been widely studied in the literature.¹² Some of these studies suggest that water plays an important role in the transport mechanism, since protons move through the ionic domains once they are interconnected with water. Unfortunately, a similar mechanism could apply for methanol transport throughout the membrane. Because of the similarities in the transport mechanism for protons and methanol, this investigation studied morphological differences in Nafion[®] membranes with the intention to control selectivities (proton conductivity over methanol permeability) and increase efficiency for DMFC applications.

More specifically, this investigation used supercritical fluids (SCFs) as a processing alternative, since the gas-like mass-transport properties of SCFs allow for better penetration into the membrane and the use of cosolvents of different chemical size, polarity, and functionality (Table I)¹³ could influence the membrane morphology, fine-tuning the physical and transport properties. SCF processed membranes were then characterized for methanol permeability and proton conductivity; the results were explained with some additional materials characterization techniques (e.g., XRD and SAXS).

EXPERIMENTAL

Materials

High-purity CO₂ (99.996% purity) was obtained from Linde Gas. Nafion[®] 117 membranes in its acid

form were obtained from Ion Power, Inc. Acetic acid (99.7% purity), acetone (HPLC grade), acetonitrile (HPLC grade), cyclohexanone (99% purity), dichloromethane (HPLC grade), ethanol (HPLC grade), isopropanol (HPLC grade), methanol (HPLC grade), tetrahydrofuran (99% purity) and water (HPLC grade), were obtained from Sigma-Aldrich Chemical Company. They were used without any further purification.

Supercritical fluid processing

Nafion[®] membranes were processed with SCF CO₂ at 40°C and 200 bars in a supercritical fluid extractor (Isco SFX 2-10) for about 1 h at a flow of ~ 0.45 mL/min. The experimental set-up consisted of a syringe pump (ISCO 260D) for constant delivery of the fluid and an extraction chamber (ISCO SFX-210), where the sample was placed at a controlled temperature (Fig. 1). The syringe pump was prefilled with CO₂ and the pressure was increased to the desired value. After the extraction cell, the extractor was equipped with a heated decompression system (restrictor) to regulate the high-pressure inside the chamber and allow for the solvent to exit the system, while accounting for the Joule-Thompson effect during decompression.

Some Nafion[®] samples were previously saturated with a cosolvent before they were processed with SCF CO₂ at 40°C and 200 bars. Also, some of the membranes were processed in two different directions: one where the SCF flowed parallel to the membrane and the other where the SCF flowed perpendicular to the plane of the membrane to study the impact of processing direction on the morphology and the resulting transport properties of the membrane.

Methanol permeability (liquid-phase)

The liquid-phase methanol permeability was measured using an FT-IR spectrophotometer (Nicolet IR 300) for each Nafion[®] membrane processed with SCF CO₂ and different cosolvents. The Nafion[®] sample was clamped on a zinc selenide ATR cell and

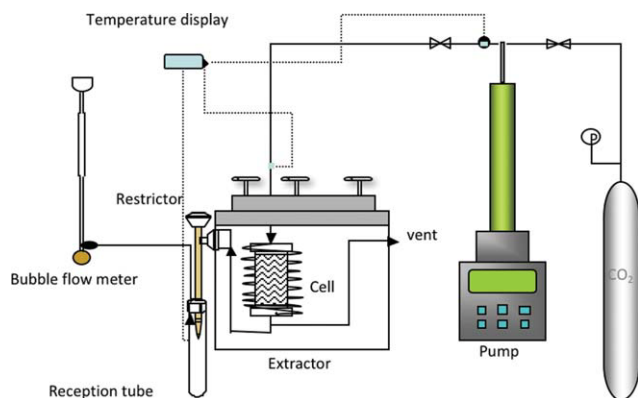


Figure 1 Supercritical fluid equipment used to process the membranes. [Color figure can be viewed in the online issue, which is available at wileyonlinelibrary.com.]

the sample was maintained wet with liquid methanol (Fig. 2). The methanol concentration on the upper part of the membrane was maintained constant with a continuous excess supply of methanol. In the lower part of the membrane the laser of the spectrophotometer measured the variation in methanol concentration that permeated through the membrane as a function of time. The methanol peak used was identified at 1016 cm^{-1} , which corresponds to the asymmetric C–O stretching not present in the original Nafion[®] membrane. An example of the evolving spectra is presented in Figure 3. A previous

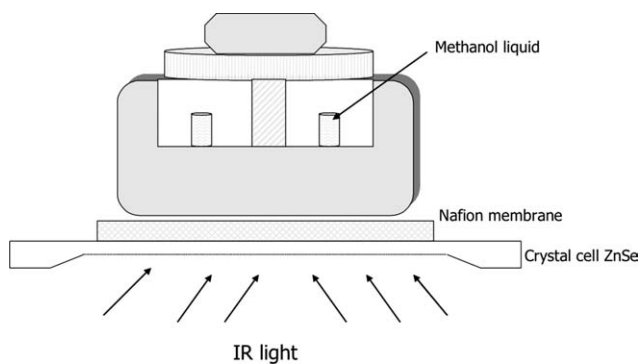


Figure 2 Experimental set-up to measure liquid-phase methanol permeabilities using an FT-IR ATR cell.

methanol concentration calibration curve versus absorbance was made with methanol solutions of known concentrations. The absorbance of the methanol peaks were correlated with the methanol concentration. Infrared spectra were recorded throughout each experiment at 30-min intervals using 32 scans and 4 cm^{-1} resolution for each collected spectrum. The results presented are the average of three replicates. Averages are presented and a propagation of error study was used to calculate the error of the measurement. Permeability measurements were validated using a side-by-side fiber-glass diffusion cell, where the Nafion[®] membrane was placed between the cells and each half-cell had a reservoir filled

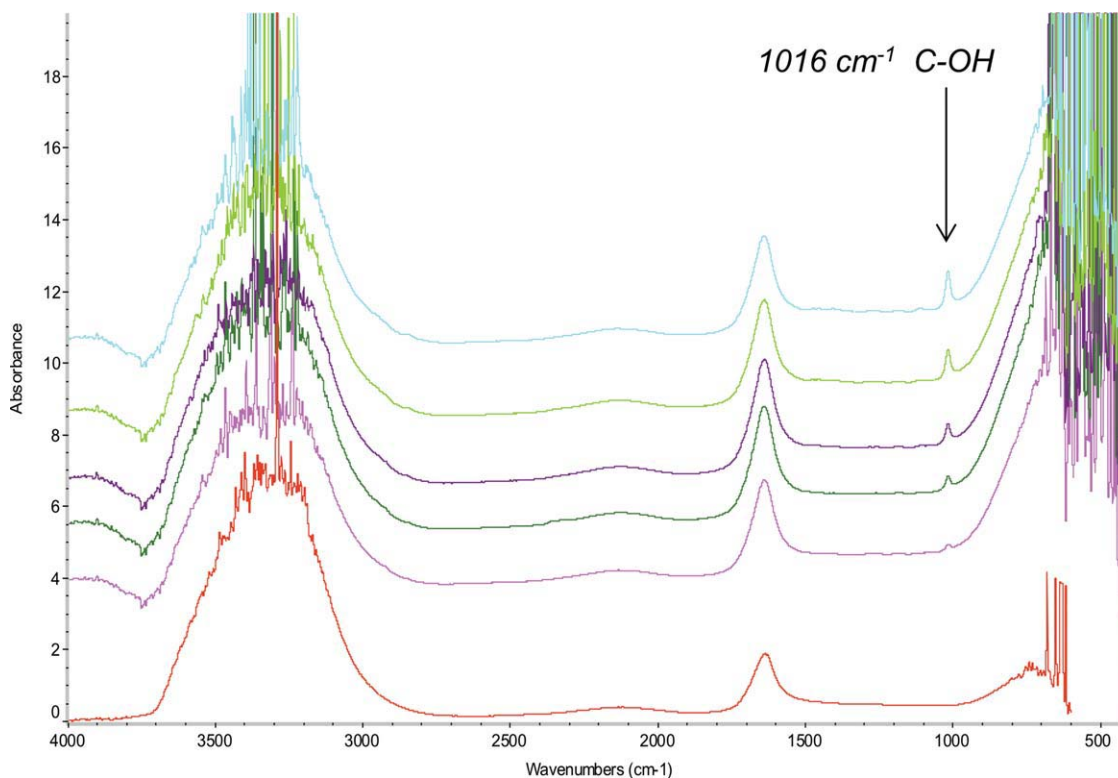


Figure 3 An example of evolving spectra with time. [Color figure can be viewed in the online issue, which is available at wileyonlinelibrary.com.]

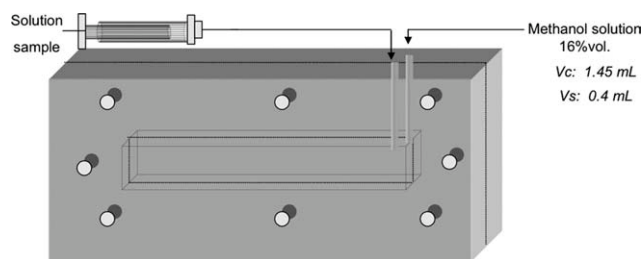


Figure 4 Diffusion cell used to measure and verify liquid-phase methanol permeabilities.

with deionized water and methanol solution respectively, (Fig. 4). The permeation of methanol was recorded from the methanol-rich to the methanol-free cell. The calculation of the methanol permeability through the membrane was obtained from the continuity equation for diffusion in plane geometry³ (eq. 1):

$$C_m(t) = \frac{PCA}{Vd} \left(t - \frac{L^2}{6D} \right) \quad (1)$$

where:

- C_m : methanol concentration below the membrane (mol/cm^3)
- C : methanol concentration in the upper part of the membrane (constant) (mol/cm^3)
- A : membrane area in contact with methanol (cm^2)
- V : membrane volume (cm^3)
- t : time (s)
- L : membrane thickness (cm)
- D : diffusion coefficient (cm^2/s)
- P : permeability (cm^2/s)

The permeability (P) was determined from the slope of the plots of methanol concentration versus time (C_m versus t). The results obtained by this method were reliable and consistent compared with the previous FTIR technique and the literature data for Nafion[®].³

Methanol permeability (vapor-phase)

Measurements of the vapor-phase methanol permeability were obtained measuring the weight loss with time throughout a glass cell with the Nafion[®] membrane on top of the cell (Fig. 5). In this experiment, the Nafion[®] membrane was the only semipermeable barrier for methanol to escape. As methanol vapor permeated across the membrane, the weight of the cell was monitored and used to determine the steady-state molar diffusion flux (J_M) and eventually the permeability. The plot of the mass of methanol that diffused across the Nafion[®] membrane as a function of the time divided by the cross-sectional area for diffusion provided the molar flux (J_M). Assuming that the

diffusion coefficient was independent of concentration and that Henry's Law applied (both valid assumptions at low concentrations of permeate), the permeability (diffusivity times the solubility) was obtained from the slope of the steady-state methanol molar diffusion flux versus time¹⁴ (eq. 2):

$$\frac{LJ_MRT}{P_M^{\text{vap}} - P_{\text{EXT}}} = P \left(t - \frac{L^2}{6D} \right) \quad (2)$$

In the expression above, L is the thickness of the membrane, J_M the molar diffusion flux of methanol, R the universal gas constant, and T the temperature of the measurement. P_M^{vap} and P_{EXT} are the methanol vapor pressure and the partial external pressure of the permeate, respectively, (in the case of organic vapors, P_{EXT} is assumed to be zero), t is the time, and D the diffusivity throughout the membrane. The slope of the plots of the left hand side of eq. (2) versus time, at steady state conditions, provides the permeability.¹⁴ Two measurements were obtained for each membrane and the results averaged; all measurements were made at $26 \pm 1^\circ\text{C}$ and under an inert constant flow of nitrogen outside the membranes.

Proton conductivity

The proton conductivity of the SCF processed samples was measured normal to the plane using AC

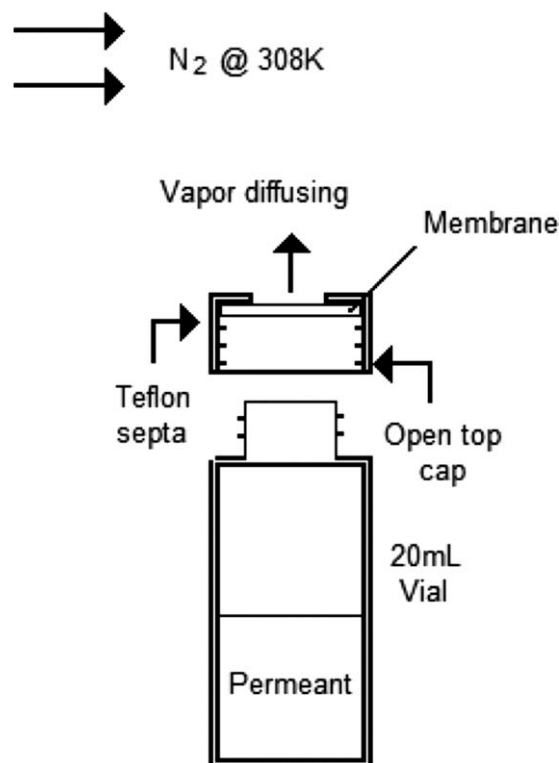


Figure 5 Experimental set-up to measure vapor-phase methanol permeabilities.

electrochemical impedance spectroscopy on a fuel cell fed by 6 mL/min of Hydrogen at $26 \pm 1^\circ\text{C}$. The measurements were carried out on a potentiostat/galvanostat (PARSTAT Model 2263). The range of frequency used was from 10 mHz up to 100 kHz (experimental limits). The higher frequencies were used to separate the membrane resistance from interfacial capacitance. The Powersuite software[®] was used to collect the impedance data (Nyquist plots), which were all semicircles. All the membranes were previously humidified by passing 250 mL of deionized water through the fuel cell prior to the measurement. The proton conductivity (σ) was calculated from the impedance data, using the following relation (eq. 3)¹⁵:

$$\sigma = \frac{L}{R_{\Omega} A} \quad (3)$$

where L and A are the thickness and area of the membrane, respectively. R_{Ω} was obtained from the low intersect of the high-frequency semicircle (Nyquist plot) on the complex impedance plane with the real component of impedance axis [Re(z)].¹⁵

X-ray diffraction

X-ray diffraction (XRD) measurements were performed using a Phillips diffractometer (Siemens D 500 Model) equipped with a Cu $K\alpha$ radiation source, a βNi filter and a graphite monochromator. No previous sample preparation was performed before the measurements, including humidity pretreatment.

Small angle X-ray scattering

Small-angle X-ray scattering (SAXS) was performed on a beamline X27C. Two-dimensional scattering patterns were collected on a pinhole-collimated system using Fujitsu image plates and read by a Fujitsu BAS 200 image plate reader. The SAXSQuant software[®] was used to reduce two dimensional data to one-dimensional intensity versus scattering vector (q) plots after background subtraction by circular averaging. The X-ray wavelength employed was 1.6 Å. The calibration standard was silver behenate and the sample distance to the detector was 210 cm.

SAXS experiments were conducted on the Nafion[®] membranes processed with SCF to determine polymer structure changes and their possible effects on the transport properties. Since the structural characterization was the focus of these analyses; for this, the intensity profiles (I versus q) were studied for each Nafion[®] membrane processed with the SCF and the different cosolvents. The samples were characterized in the plane of the film. The scattering vector, q , was defined as (eq. 4):

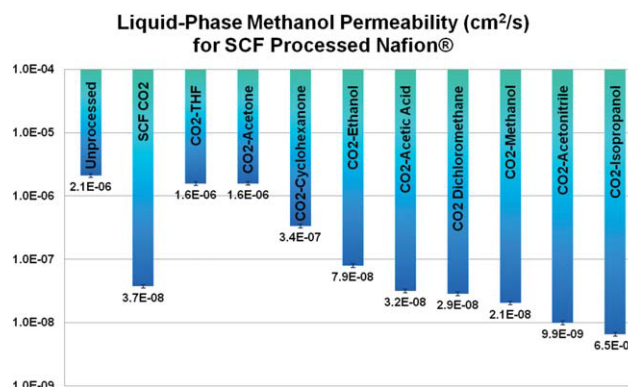


Figure 6 Liquid-phase methanol permeabilities for nafion[®] membranes processed with SCF CO₂ aided with different cosolvents. [Color figure can be viewed in the online issue, which is available at wileyonlinelibrary.com.]

$$q = \frac{4\pi \sin(\theta)}{\lambda} \quad (4)$$

where θ and λ are scattering angle and wavelength, respectively.

RESULTS AND DISCUSSION

Liquid-phase methanol permeability of Nafion[®] membranes treated with SCF CO₂ and cosolvents are presented in Figure 6 and Table II. The results for unprocessed Nafion[®] compare well with values of permeability reported in the literature.³ The error bars correspond to the variation in the repeated measurements. From Figure 6 one can observe that the permeability of methanol through Nafion[®] was significantly reduced after SCF CO₂ processing (two orders of magnitude). The use of some small polar cosolvents (e.g., acetonitrile and isopropanol) decreased the methanol permeability even further. SCF processing with some polar aprotic cosolvents (i.e., acetone and THF) had the smallest effect in the methanol permeability of Nafion[®] membranes.

Methanol swelling measurements were made for the unprocessed membranes (55.6%) and for the SCF CO₂ processed membranes (50.2%). Although the solubility was reduced upon SCF CO₂ processing, the reduction in permeability is significantly larger and therefore is not simply a Thermodynamic effect. One possible explanation for the reduction of the liquid-phase methanol permeability could be the affinity of the perfluorinated groups of the Nafion[®] membrane to the SCF CO₂. The polarizability per volume of SCF CO₂ is very similar to that of perfluorinated groups in the range of temperature and pressures studied.¹⁶ The decrease in methanol permeability could also be attributed to variations in the free volume of the polymer matrix. It has been found that the permeability can be well correlated to

TABLE II
 (a) Liquid-Phase Methanol Permeability For SCF Processed Nafion[®]; (b) Vapor-Phase Methanol Permeability for SCF Processed Nafion[®]; (c) Proton Conductivity for SCF Processed Nafion[®]

(a) Processing solvent	$P_m \times 10^9 \{ \text{cm}^2/\text{s} \}$
Unprocessed	2100 ± 100
CO ₂	37 ± 3
CO ₂ + THF	1600 ± 100
CO ₂ + Acetone	1600 ± 100
CO ₂ + Cyclohexanone	340 ± 20
CO ₂ + Ethanol	79 ± 4
CO ₂ + Acetic Acid	32 ± 2
CO ₂ + Dichloromethane	29 ± 2
CO ₂ + Methanol	21 ± 1
CO ₂ + Acetonitrile	9.9 ± 0.6
(b) Processing solvent	$P_m \times 10^2 \{ \text{cm}^2/\text{s} \}$
Unprocessed	9.1 ± 0.6
CO ₂	7.8 ± 0.6
CO ₂ + THF	2.9 ± 0.4
CO ₂ + Acetone	7.1 ± 0.5
CO ₂ + Cyclohexanone	9.4 ± 0.6
CO ₂ + Ethanol	8.7 ± 0.5
CO ₂ + Acetic Acid	7.3 ± 0.5
CO ₂ + Dichloromethane	6.7 ± 0.6
CO ₂ + Methanol	6.2 ± 0.5
CO ₂ + Acetonitrile	6.3 ± 0.5
CO ₂ + Isopropanol	5.7 ± 0.4
(c) Processing solvent	$\sigma \{ \text{S}/\text{cm} \}$
Unprocessed	0.09 ± 0.01
CO ₂	0.08 ± 0.01
CO ₂ + THF	0.03 ± 0.005
CO ₂ + Acetone	0.07 ± 0.008
CO ₂ + Cyclohexanone	0.09 ± 0.012
CO ₂ + Ethanol	0.09 ± 0.008
CO ₂ + Acetic Acid	0.07 ± 0.01
CO ₂ + Dichloromethane	0.07 ± 0.007
CO ₂ + Methanol	0.06 ± 0.006
CO ₂ + Acetonitrile	0.06 ± 0.006
CO ₂ + Isopropanol	0.06 ± 0.005

the free volume available in the system.¹⁷ Although the transport of methanol is also from sulfonic group to sulfonic group, the methanol molecules only diffuse through the free volume in the polymeric matrix and thus the diffusion can be described using a statistical description of this free volume.

To corroborate the previously observed trends in the liquid-phase, vapor-phase methanol permeabilities were measured and the results presented in Figure 7 and Table II. The vapor-phase results show a similar trend to the liquid-phase permeability results; the SCF processing inhibits the vapor phase permeation and some cosolvents were more significant than others retarding the transport of methanol vapor through the membrane. The difference between the vapor-phase and the liquid-phase results could be attributed to the role of water in the vapor-phase versus liquid-phase transport, which was not fully studied in this investigation, and the morphological differences within the membranes.

Figure 8 and Table II presents the proton conductivity of the Nafion[®] samples processed with SCFs.

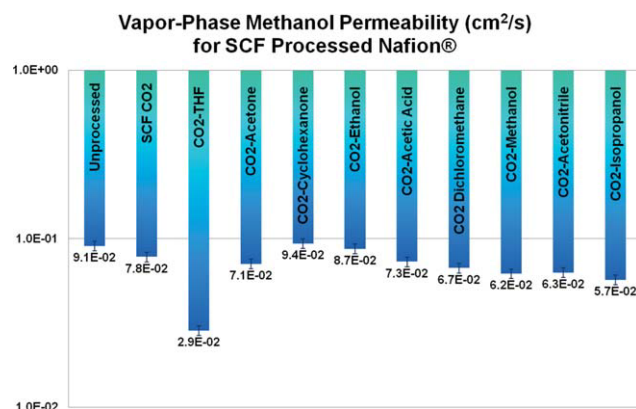


Figure 7 Vapor-phase methanol permeabilities for nafion[®] membranes processed with SCF CO₂ aided with different cosolvents. [Color figure can be viewed in the online issue, which is available at wileyonlinelibrary.com.]

The error bars correspond to the variation in the repeated measurements, which was 10%. The use of some polar cosolvents (cyclohexanone and ethanol), had the smallest effect on the proton conductivity of Nafion[®]. The other cosolvents, including pure SCF CO₂ had an expected reduction in the proton conductivity from 4 to 69%. Since the proton conductivity of cyclohexanone was unusually and consistently the highest, additional material characterization was performed to understand this phenomenon.

Since both methanol permeability and proton conductivity decreased for most of the membranes studied, selectivities (proton conductivity over methanol permeability) were calculated and the normalized values (normalized with unprocessed Nafion[®]) are presented for comparison purposes (Fig. 9). SCF CO₂ processing with the aid of isopropanol and acetonitrile had the largest effect on the selectivity of Nafion[®] membranes, perhaps due of their unique combination of cosolvent size and physical properties (Table I). The use of THF as a cosolvent had a

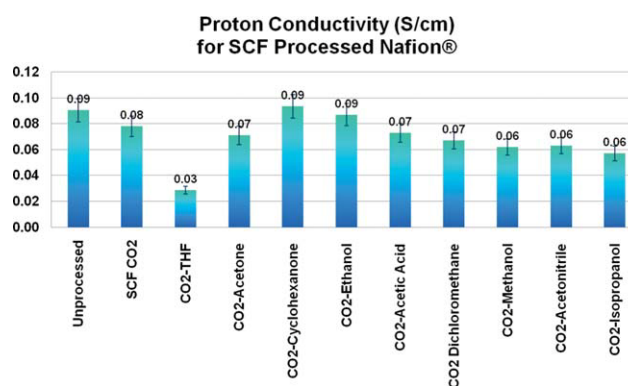


Figure 8 Proton conductivity for nafion[®] membranes processed with SCF CO₂ aided with different cosolvents. [Color figure can be viewed in the online issue, which is available at wileyonlinelibrary.com.]

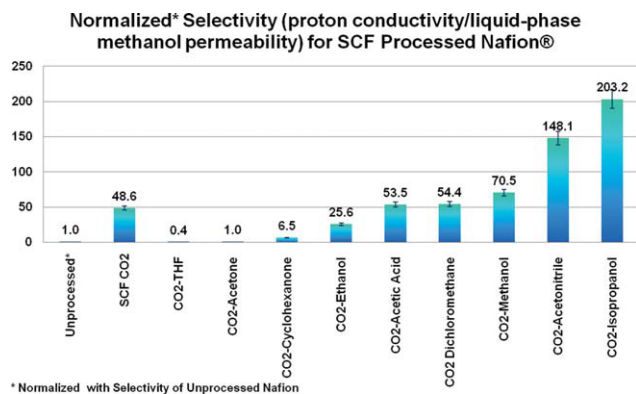


Figure 9 Normalized selectivities (proton conductivity/methanol permeability) for nafion® membranes processed with SCF CO₂ aided with different cosolvents. [Color figure can be viewed in the online issue, which is available at wileyonlinelibrary.com.]

negative net effect on the normalized selectivity of Nafion®, perhaps due to its unique size and polarity.

XRD results for some of the membranes studied are shown in Figures 10–12. Figure 10 compares the XRD results for unprocessed Nafion® with Nafion® processed with SCF CO₂ and with SCF CO₂ and isopropanol (the largest normalized selectivity). Unpro-

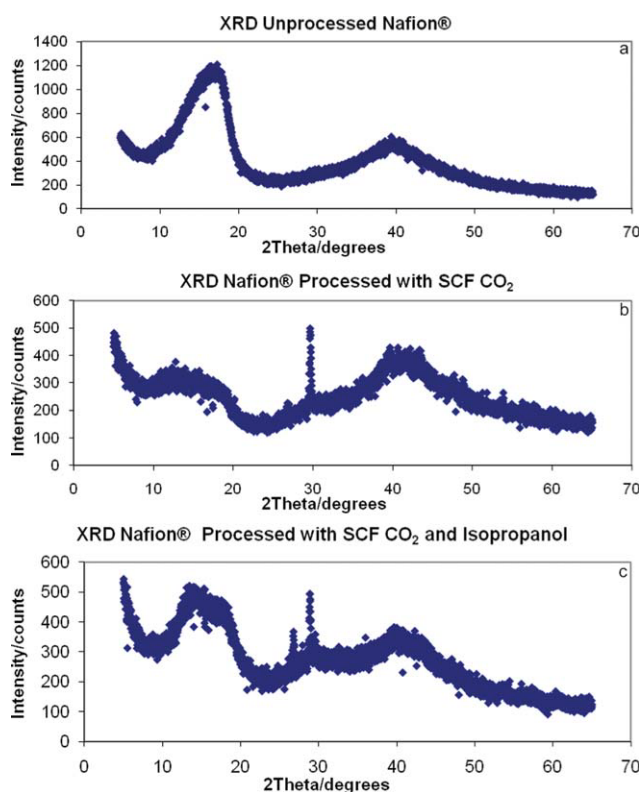


Figure 10 XRD of nafion® membranes: (a) Corresponds to Unprocessed Nafion®, (b) corresponds to Nafion® processed with SCF CO₂, (c) Corresponds to Nafion® Processed with SCF CO₂ and Isopropanol. [Color figure can be viewed in the online issue, which is available at wileyonlinelibrary.com.]

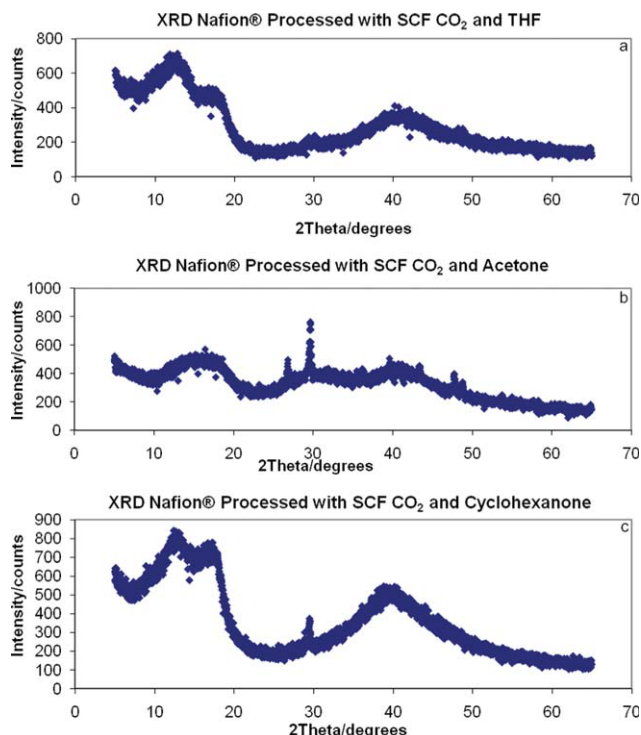


Figure 11 XRD of nafion® membranes: (a) Corresponds to nafion® processed with SCF CO₂ and THF, (b) corresponds to nafion® processed with SCF CO₂ and acetone, (c) Corresponds to nafion® processed with SCF CO₂ and cyclohexanone. [Color figure can be viewed in the online issue, which is available at wileyonlinelibrary.com.]

cessed Nafion® contains a crystalline peak ($2q = 17.6^\circ$) and a broad amorphous halo centered on $2q = 40^\circ$. The sample processed with SCF CO₂ shows a vanishing pattern of the crystalline region at $2q = 17.6^\circ$, which could be related to a decrease in the free volume and therefore could explain the reduction in the methanol permeability. The use of cosolvents with SCF CO₂ (Figs. 10–12) produce unique structural modifications which in addition to changes in the crystallinity and the free-volume of Nafion®, some of them also influence the hydrophilic regions of the membrane. For example, the samples processed with SCF CO₂ with cosolvents isopropanol and acetone show a significant difference in a crystalline peak around $2q = 30^\circ$; other cosolvents show other changes. In general terms XRD results suggest that processing with SCF CO₂ plus cosolvents influences: the free volume, the hydrophilic domains, and the changes in the crystalline region(s) of the membrane. These results are in agreement with a recent rod-model^{18,19} for Nafion® that suggests the sulfonic groups are arranged into crystal-like rods and the use of cosolvents of unique specific interactions and entropic contributions (produced by the shape and size differences), produces unique changes in the crystallinity of the processed membrane.

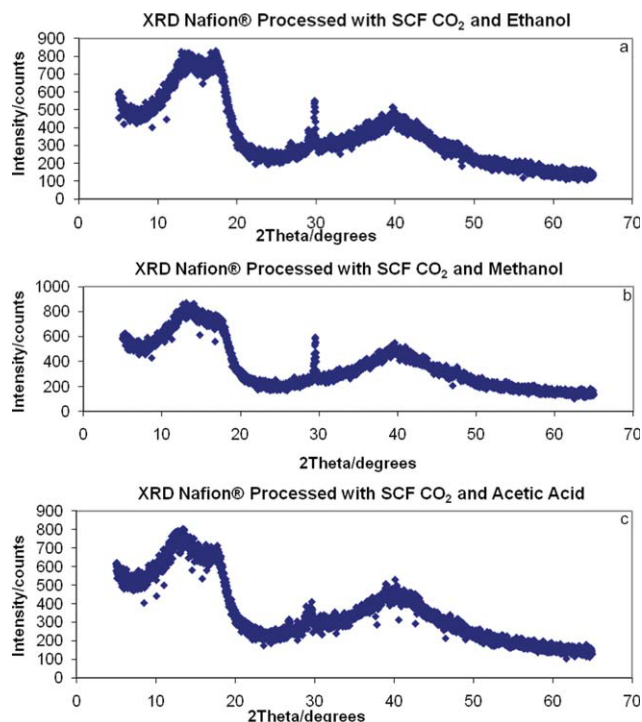


Figure 12 XRD of nafion[®] membranes: (a) Corresponds to nafion[®] processed with SCF CO₂ and ethanol, (b) corresponds to Nafion[®] processed with SCF CO₂ and methanol, (c) corresponds to nafion[®] processed with SCF CO₂ and acetic acid. [Color figure can be viewed in the online issue, which is available at wileyonlinelibrary.com.]

Most of the samples were processed using SCF CO₂ with parallel flow through the membrane, while transport properties were measured perpendicular to the membrane (Fig. 13). Since Elabd and coworkers³ found variations in the transport properties with the direction of the measurement, this investigation decided to process one Nafion[®] sample with SCF CO₂ flowing perpendicular through the membrane and compare it with the parallel flow study. The sample processed using perpendicular flow did not show a significant change in the transport properties previously presented, as those processed with parallel flow through the membrane. The XRD results for these two processing schemes are presented in Figure 14. The results for the samples processed with the SCFs using perpendicular flow showed very little change in the region of $2q = 17.6^\circ$, compared with the parallel flow measurement. In addition, the perpendicular flow study did not show the additional crystalline peak around $2q = 30^\circ$ also observed in many of the samples with very good selectivities. The results for the different flow configurations confirm the anisotropic nature of Nafion^{®20} and suggest that the perpendicular flow cannot influence the free-volume and the crystallinity as the parallel flow processing, perhaps because the orientation of the polymeric chains and the rod-like crystals in the Nafion[®] nanostructure.

SAXS profiles for Nafion[®] membranes are presented in Figure 15. SAXS profiles show two major peaks, the first peak, at the lowest scattering vector (around 0.45 nm^{-1}), has been attributed to the hydrophobic polymer matrix (perfluorinated groups) of the Nafion[®] membrane.^{21–23} The perfluorinated and perfluorovinylether groups aggregate to form clusters and the dimension of these is controlled by the polymer chain rigidity, the distance between ionic groups along the polymer chain, and the steric hindrance of the latter, creating some geometrical packing constraints. Significant changes were observed for this peak upon SCF CO₂ processing with and without cosolvents. The processing with SCF minimized the interfacial energy taking into account the geometrical packing constraints induced by the residual cosolvent located at the interface.

The second peak of the profiles, which are showed at higher values of the scattering vector (around 1.8 nm^{-1}), is often called the ionomer peak,¹⁹ and is related to the sulfonic groups present in Nafion[®], which play an important role in the transport of protons through the membrane. The most significant variation in this region occurs with the use of SCF CO₂ and the cosolvent cyclohexanone. This variation in the ionomer peak for cyclohexanone agrees with the unusually high proton conductivity obtained in the previous section, which seem to indicate no net effect over the interconnection of sulfonic groups responsible for the transport of protons.

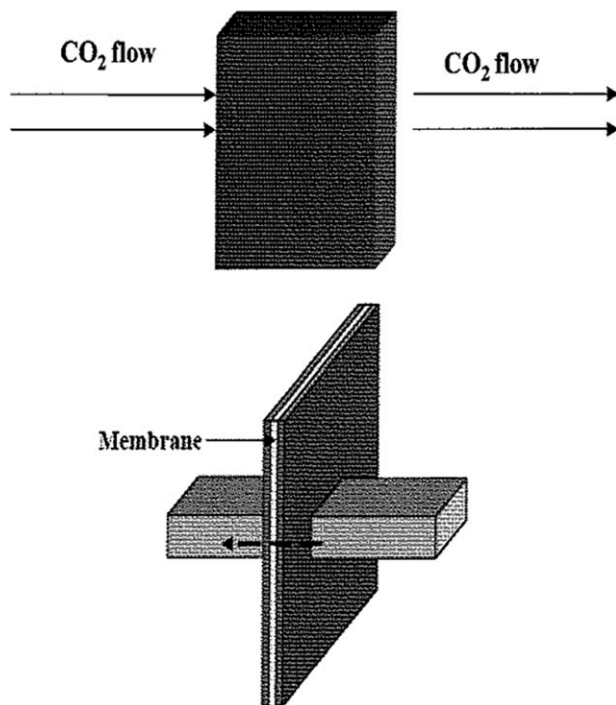


Figure 13 Upper: schematic representation of SCF CO₂ flow during processing (parallel flow). Bottom: schematic representation of direction of proton conductivity and methanol permeability measurements (perpendicular flow).

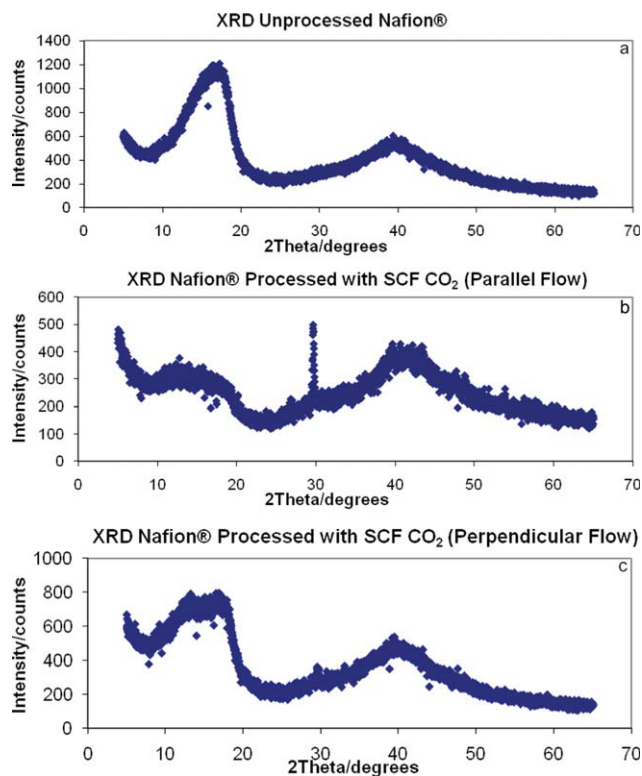


Figure 14 XRD of nafion[®] membranes: (a) Corresponds to unprocessed nafion[®], (b) corresponds to nafion[®] processed with SCF CO₂ in parallel flow, (c) corresponds to nafion[®] processed with SCF CO₂ in perpendicular flow. [Color figure can be viewed in the online issue, which is available at wileyonlinelibrary.com.]

Because of the perfluorinated nature of the polymer matrix in Nafion[®], SAXS profiles lead to a high level of scattered intensities. These scattered inten-

sities can be due to ionic cluster aggregates connected by small channels. Since the unprocessed Nafion[®] has high proton conductivity, it can be inferred that a percolation (through small connecting ionic channels) should occur in the membranes to transport the methanol. The broad halos showed at the XRD and SAXS results may be due to the scattering from large crystal, or the presence of small crystalline structure, or from the amorphous region. On the other hand the scattering patterns presented in XRD and SAXS can be attributed to changes in the hydrophilic ionic domains and a reordering of the perfluoroether side chains.

The Nafion[®] membrane treated with SCF showed a decrease in crystallinity, which suggests a reduction in the absorption of alcohols and water by the membrane. Methanol and water have the ability to hydrogen bond with itself and to interact strongly with the polymer. The structural changes that cause the morphological modifications also affect the polymer–water and polymer–methanol interactions. This way the methanol transport could be influenced by not only the crystallinity, but also by the hydrophilicity and the free volume of the polymer.

Figure 15 also shows that the processed samples present a similar scattering pattern, which tends to correspond to ordered morphology. The interplanar or Bragg spacing, which has been interpreted as an average domain spacing or size, can be calculated from Bragg’s law (eq. 5):

$$d_{lam} = \frac{2\pi}{q^*} \tag{5}$$

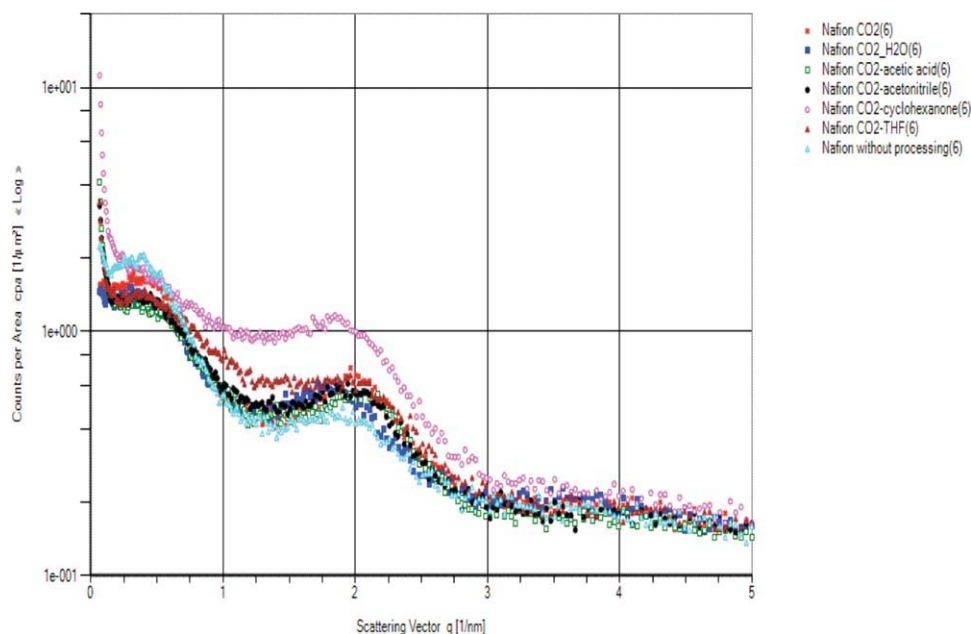


Figure 15 SAXS profiles for nafion[®] membranes processed with SCFs. [Color figure can be viewed in the online issue, which is available at wileyonlinelibrary.com.]

TABLE III
Bragg Spacing For Nafion[®] Membranes Treated with SCF and Cosolvents

Processing solvent	<i>d</i> (nm)
Unprocessed	13.96
CO ₂	12.82
CO ₂ + Acetic Acid	12.88
CO ₂ + Acetonitrile	12.67
CO ₂ + Cyclohexanone	13.06
CO ₂ + THF	12.74

The Bragg spacing, d_{1am} , is determined from the maximum in the first order reflection, q^* . The d_{1am} values calculated are listed in Table III and are similar for most of the processing solvents. These values range from 12.7 to 14.0 nm with no apparent trend with the cosolvents used for processing. The highest value for d_{1am} was obtained for the unprocessed membrane suggesting that indeed SCF processing reduced the free-volume responsible for the transport through the membrane.

CONCLUSIONS

Nafion[®] membranes processed with SCF CO₂ showed a reduction in the liquid and vapor phase methanol permeability, while proton conductivity was only slightly reduced. The use of polar cosolvents with SCF CO₂ also reduced the methanol permeability while maintaining the proton conductivity of some of the membranes. The best selectivity (proton conductivity over methanol permeability) normalized with unprocessed Nafion[®] was obtained using SCF CO₂ and isopropanol; however, the use of other cosolvents such as ethanol reduced the methanol permeability by two orders of magnitude while the proton conductivity was only reduced by 4%. Each cosolvent produced a unique combination of effects led by morphological differences within the membrane. One probable explanation to this observed behavior is that aided by the high diffusivity of the SCF CO₂ and the CO₂-philic nature of perfluorinated groups, the polar cosolvents are pene-

trating the membrane more easily changing the crystallinity of the membrane, which is related to the free-volume and therefore the resulting transport properties of the membrane.

Different flow arrangements (parallel versus perpendicular flow) were studied, but only parallel flow processing achieved the significant changes in transport properties. Processing with perpendicular flow did not influence the free-volume and the crystallinity as parallel flow processing.

References

- Ge, J.; Liu, H. *J Power Sources* 2005, 142, 55.
- Ahmad, H.; Kamarudin, S. K.; Hasran, U. A.; Daud, W. R. W. *Int J Hydrogen Energy* 2010, 35, 2160.
- Elabd, Y. A.; Napadensky, E.; Sloan, J. M.; Crawford, D. M.; Walker, C. W. *J Membr Sci* 2003, 217, 227.
- Li, X.; Roberts, E. P. L.; Holmes, S. M.; Zholobenko, V. *Solid State Ionics* 2007, 178, 1248.
- Affoune, A. M.; Yamada, A.; Umeda, D. M. *J Power Sources* 2005, 148, 9.
- Kim, D. S.; Liu, B.; Guiver, M. D. *Polymer* 2006, 47, 7871.
- Karlsson, L. E.; Jannasch, P. *J Membr Sci* 2004, 230, 61.
- Wycisk, R.; Chisholm, J.; Lee, J.; Lin, J.; Pintauro, P. N. *J Power Sources* 2006, 163, 9.
- Ainla, A.; Brandell, D. *Solid State Ionics* 2007, 178, 581.
- Elabd, Y. A.; Napadensky, E. *Polymer* 2004, 45, 3037.
- Miyake, N. *J Electrochem Soc* 2001, 148, A898.
- Miyake, N. *J Electrochem Soc* 2001, 148, A905.
- Poling, B. E.; Prausnitz, J. M.; O'Connell, J. P. *The Properties of Gases and Liquids*, 5th ed., McGraw-Hill: New York, 2000.
- Poley, L. H.; Vargas, H. *Polimeros: Ciencia e Tecnologia* 2005, 15, 22.
- Grossi, N.; Espuche, E.; Escoubes, M. *Separation Purification Technol* 2001, 22, 255.
- Johnston, K. P.; Kim, S.; Combes, J. *Supercritical Fluid Sci Technol. ACS Symp Series* 1989, 406, 52.
- Cohen, M. H.; Turnbull, D. *J Chem Phys* 1959, 31, 1164.
- Mauritz, K. A.; Moore, R. B. *Chem Rev* 2004, 104, 4535.
- Gebel, G.; Diat, O. *Fuel Cells* 2005, 5, 261.
- Gardner, C. L.; Anantaraman, A. V. *J Electroanal Chem* 1998, 449, 209.
- Page, K. A.; Landis, F. A.; Phillip, A. K.; Moore, R. B. *Macromolecules* 2006, 39, 3939.
- Grerke, T. D.; Munn, G. E.; Wilson, F. C. *J Polym Sci, Polym Phys Ed* 1981, 19, 1687.
- Fujimura, M.; Hashimoto, T.; Kawai, H. *Macromolecules* 1981, 14, 1309.